Rev.Adv.Mater.Sci. 10 (2005) 133-137

STRAIN HARDENABILITY OF ULTRAFINE GRAINED LOW CARBON STEELS PROCESSED BY ECAP

Kyung-Tae Park[1], Chong Soo Lee[2] and Dong Hyuk Shin[3]

[1]Division of Advanced Mater. Sci. and Eng, Hanbat Nat'l Univ., Taejon 305-719, Korea
[2]Department of Mater. Sci. and Eng, POSTECH, Pohang, 790-784, Korea
[3]Department of Metall. and Mater. Sci., Hanyang University, Ansan, 425-791, Korea

Received: May 02, 2005

Abstract. Room temperature tensile properties of ultrafine grained (UFG) low carbon steels prepared by using equal channel angular pressing (ECAP) and post heat treatment are reviewed, focusing on the restoration of their strain hardenability. The utilization of nano-sized vanadium carbide particles was found to be less effective on improving strain hardenability of UFG ferrite/pearlite steel. By contrast, UFG ferrite/martensite dual phase steel exhibited an excellent combination of ultrahigh strength, large uniform elongation and even extensive strain hardenability.

1. INTRODUCTION

The room temperature tensile properties of ultrafine grained (UFG) low carbon ferrite/pearlite (F/P) steels [1] are manifested by ultrahigh strength with very limited strain hardening, as typical in other UFG materials. Since strain hardenability directly influences the formability, recent studies on fabrication of UFG materials are devoted to the restoration of their strain hardenability, and therefore several promising suggestions are available. The representatives are the utilization of uniform distribution of nano-sized second phase particles, strain gradient plasticity, the bimodal grain size distribution, their inherent high strain rate sensitivity at low strain rates, *etc* [2-4]. Among these approaches, the first two are relatively simple to apply to the steel in terms of the easiness of processing since they are already in application for the coarse grained steels: i.e. microalloyed steels for the first one, and dual phase steels for the second one. Accordingly, in the present investigation, UFG low carbon vanadium(V)-alloyed steel and ferrite/martensite (F/M) dual phase (DP) steel were prepared by equal channel angular pressing (ECAP) [5] and their tensile properties were examined with a special focus on strain hardenability.

2. EXPERIMENTAL

UFG V-alloyed steel. The ingot of Fe-0.15C-0.25Si-1.12Mn-0.34V-0.012N (in wt.%) was homogenized at 1523K for 1 hr and size-rolled. After machining the rods of 10 mm diameter and 130 mm length, the rods were austenitized at 1473K for 1 hr, direct-quenched at 873K, maintained for 4 hrs and air-cooled for V precipitates to form during ECAP and/or subsequent annealing treatment. ECAP was carried out at 623K up to 4 passes with route C (180°

Corresponding author: Kyung-Tae Park, e-mail: ktpark@hanbat.ac.kr

sample rotation between the pass): the present ECAP die was designed to yield an effective strain of ~ 1 per pass. The ECAPed samples were further annealed at 933K ·1 hr.

UFG F/M DP steel. A Fe-0.15%C-0.25%Si-1.1%Mn (in wt.%) steel was austenitized at 1473K for 1 hr and then air-cooled. Then, ECAP was conducted at 773K up to 4 passes with route C. The relatively high ECAP temperature was selected in order to minimize grain growth of retained ferrite during subsequent intercritical annealing. Intercritical annealing of 1013K·10 min followed by water quenching was undertaken on the ECAPed samples. For the purpose of comparison, coarse grained dual phase steel (CG-DP steel) was prepared by the identical intercritical annealing without ECAP.

Tensile tests and microstructure observation. Tensile specimens with a gage length of 25.4 mm were machined from both UFG V-alloyed steel and UFG F/M DP steel. Room temperature tensile tests were carried out at an initial strain rate of $1Ч10^{-3}$ s^{-1} on an Instron machine operating at a constant crosshead speed. The raw tensile data were smoothed by the adjacent 5 points averaging method in order to avoid the undesired data scattering for calculating the strain hardening rate. The size and volume fraction of ferrite and martensite in the UFG F/M DP steel were measured by scanning electron microscope (SEM, JEOL 6330F with 20 kV) and an image analyzer. The substructures were examined by transmission electron microscope (TEM, JEOL 2010 with 200 kV). For TEM observation, thin foils were prepared by a twin-jet polishing technique using a mixture of 20% perchloric acid and 80% methanol at an applied potential of 40 V and at 233K.

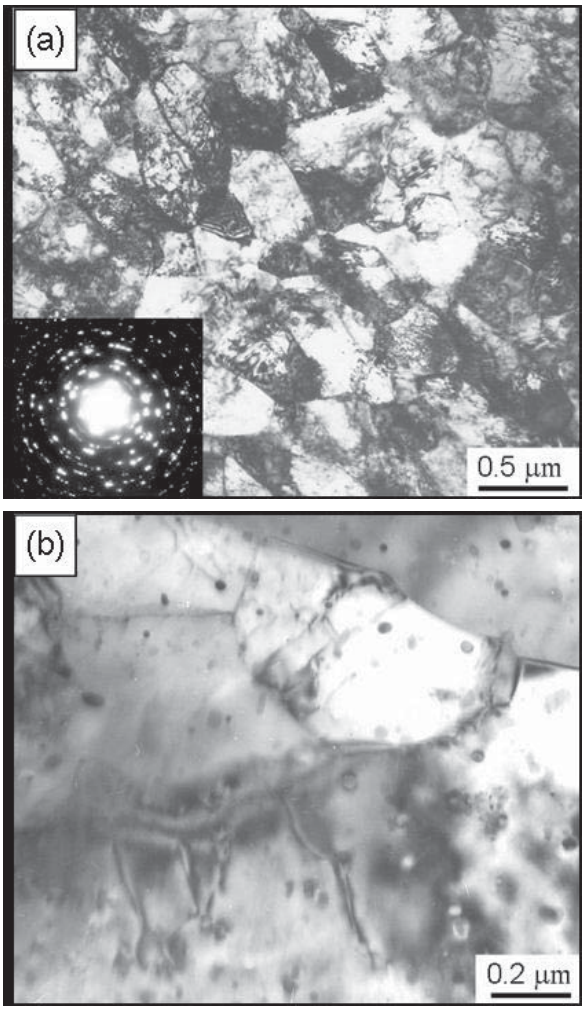

Fig. 1. (a) TEM micrograph of ferrite grains of the UFG V-alloyed steel. (b) TEM replica image showing the distribution and size of V carbides at the ferrite grain interior of the UFG V-alloyed steel.

3. RESULTS AND DISCUSSION

3.1. Microstructure

As shown in Fig. 1, the microstructures of the V-alloyed steel are characterized by (a) the grain size of 0.2~0.3 μm, (b) ill-defined grain boundaries, (c) dense dislocation debris, (d) near-ring type SADP, and (e) random distribution of V carbides of 10~30 nm.

The microstructure of UFG F/M DP steel consisted of equiaxed ferrite grains and uniformly distributed martensite islands (Fig. 2a). SEM micrograph with higher magnification (Fig. 2b) revealed that martensite was in an isolated blocky type. Both ferrite grain size and martensite island size were ~0.8 μm and the martensite volume fraction was about 28%. Similar to the coarse grained counterparts, a very high density of dislocations associated with transformation accommodation was observed in the ferrite grain adjacent to martensite (Fig. 2c).

3.2 . Tensile properties

UFG V-alloyed steel. The representative nominal stress-strain curves for the V-alloyed steel are shown in Fig. 3a. Before ECAP (curve a), the V-alloyed steel exhibited continuous yielding and moderate strain hardening. For the as-ECAPed state (curve b), the yield strength reached over 900 MPa, almost twice of that before ECAP, but very little uniform elongation with no strain hardening was obtained. The V-alloyed steel annealed at 933K for 1hr after ECAP

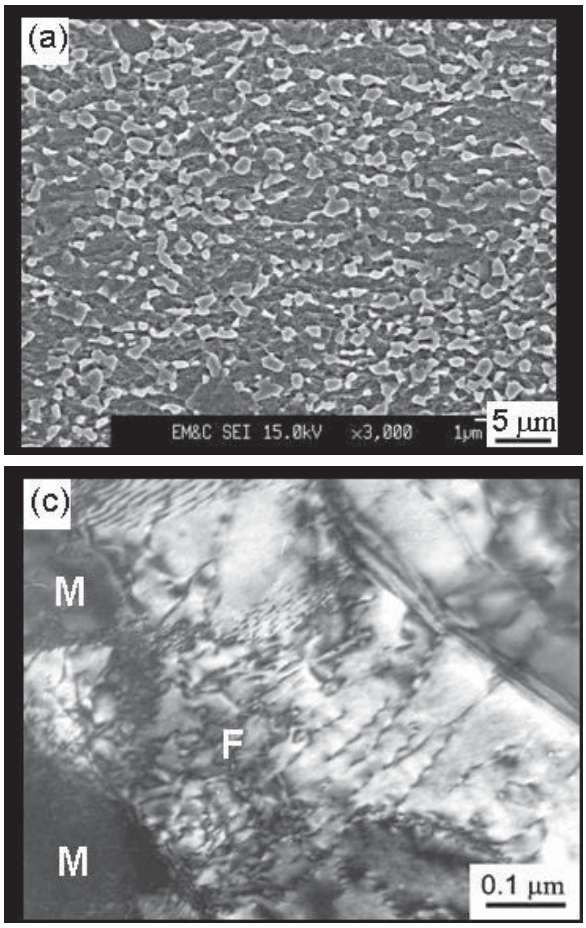

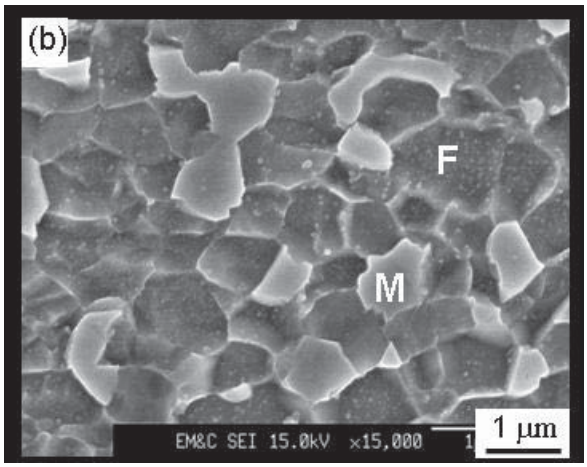

Fig. 2. (a) SEM micrograph of the UFG F/M DP steel. (b) Enlarged SEM micrograph showing the distribution and size of martensite islands of the UFG F/M DP steel. (c) Transformation accommodation dislocations with a high density in the vicinity of martensite islands.

(curve c) revealed (a) the YS, UTS, and flow stress were much superior to those of the sample before ECAP (curve a), (b) the uniform as well as total elongations were similar to those of the sample before ECAP, and (c) strain hardening was improved a little compared to the as-ECAPed state (curve b). By applying the Hollomon equation of $\sigma = K\varepsilon^N$, the strain hardening exponent of curves a (before ECAP) and c (ECAP+annealing) was estimated as ~0.15 and ~0.09, respectively. These results show that the use of nano-sized second phase particles for improving strain hardenability of UFG ferrite/pearlite steels is not effective in spite of intensive interaction between dislocations and particles as shown in Fig. 3b.

UFG F/M DP steel. The representative engineering and true stress-strain (S-e and s-e) curves of UFG F/M DP steel are presented in Figs. 4a and 4b, respectively. For the purpose of comparison, those of coarse grained (CG) F/M DP steel are superimposed in the same plots. The tensile data of both dual phase steels are listed in Table 1 along with their microstructural parameters. The two findings are noticeable. First, unlike the UFG ferrite-pearlite steel showing no strain hardening, the σ-ε curve of

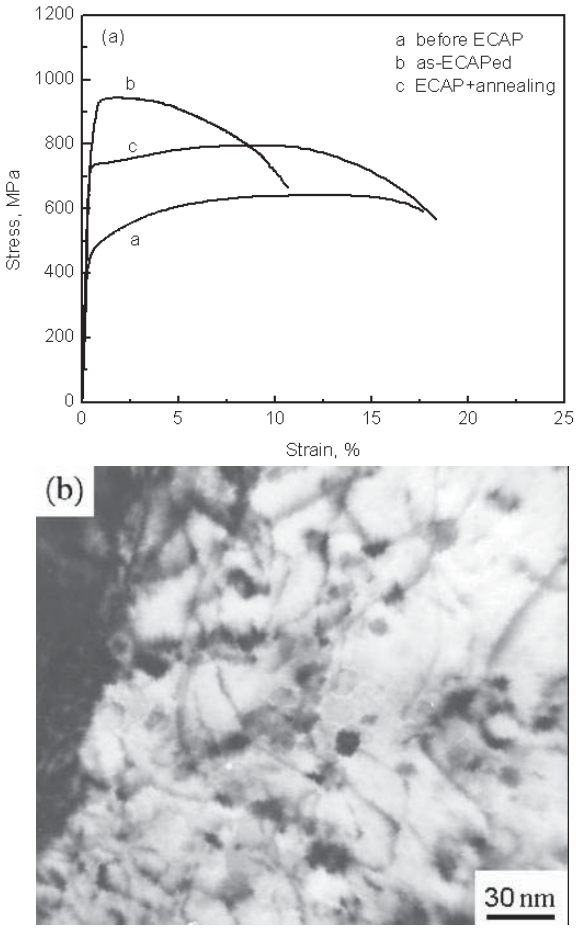

Fig. 3. (a) Representative nominal stress-strain curves of the V-alloyed steel: curve a - before ECAP, curve b - after ECAP, and curve c - annealed at 933K for 1 hr after ECAP. (b) TEM micrograph showing the interaction between V carbides and dislocations in the V-alloyed steel (ECAP + annealing) after tensile test.

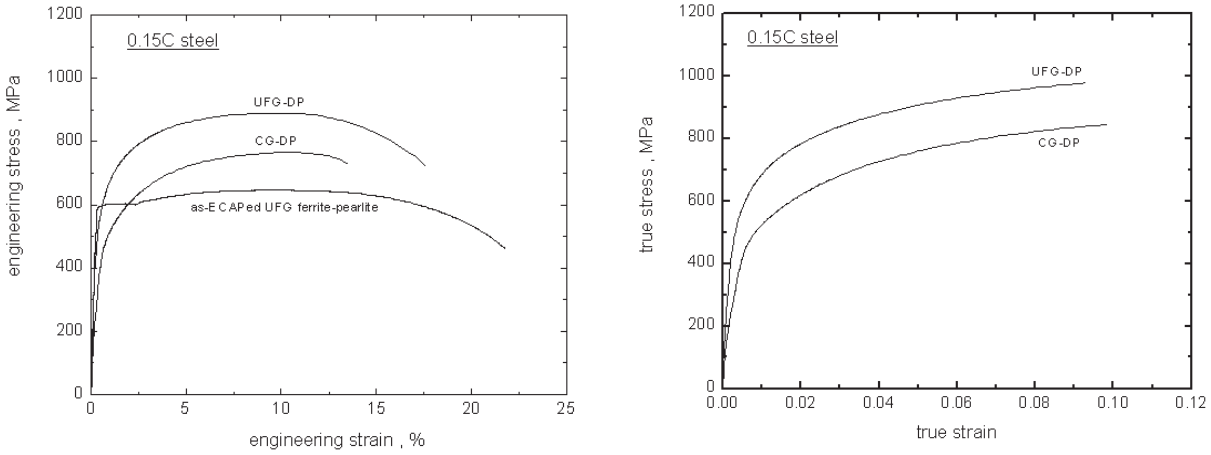

Fig. 4. The stress-strain curves of the present dual phase steels: (a) the S-e curves; (b) the σ–ε curves.

UFG F/M DP steel is similar to that of CG F/M DP steel in terms of continuous yielding and rapid strain hardening at the initial stage of plastic deformation. This finding suggested that strain hardening of dual phase steels is less affected by the ferrite grain size. By contrast, the as-ECAPed UFG ferrite-pearlite steel, of which S-e curve is included in Fig. 4a, exhibited discontinuous yielding and negligible strain hardening. Most dislocations generated by ECAP are annihilated by static recovery during intercritical annealing and they are replaced by newly formed mobile dislocations for transformation accommodation during subsequent quenching, consequently resulting in continuous yielding, rapid strain hardening with less dependence on the ferrite grain size. Second, yield strength (σ_{YS}) and ultimate tensile strength (σ_{UTS}) of UFG F/M DP steel were much higher than those of CG F/M DP steel in spite of almost the same ε_u and even larger engineering total elongation (e_t). In addition, the yield ratio (σ_{YS}/σ_{UTS}) of both dual phase steels was the same. Generally, the strength of dual phase steels linearly increases with increasing the martensite volume fraction (V_f) and obeys the Hall-Petch equation in terms of the ferrite grain size (d_m). Accordingly, it is certain that higher strength of UFG F/M DP steel is attributed to not only ultrafine d_m but also larger V_f compared to those of CG F/M DP steel.

Of the analytical methods describing the strain hardening behavior of metals and alloys, the modified Crussard-Jaoul (C-J) analysis [6] based on the Swift equation [7] is known to best describe that of DP steels [8]. The Swift σ-ε relationship is expressed as

$$\varepsilon = \varepsilon_0 + k\sigma^m, \tag{1}$$

where ε and σ are the true strain and stress, respectively, m is the strain hardening exponent, and ε_o and k are materials constants. The differentiation of the logarithmic form of Eq. (1) gives

$$\ln\frac{d\sigma}{d\varepsilon} = (1-m)\ln\sigma - \ln(km). \tag{2}$$

Then, m can be obtained from the slope, (1-m), of the ln ($d\sigma/d\varepsilon$) versus lnσ curve. Such a plot is depicted in Fig. 5. This figure reveals several findings. First, UFG F/M DP steel exhibited the two

Table 1. Tensile properties of the present DP steels with their microstructural parameters.

steels	V_m (%)	d_m (μm)	d_f (μm)	σ_{YS} (MPa)	σ_{UTS} (MPa)	ε_u (%)	e_t (%)	YS/UTS
UFG-DP	28.2	0.8	0.8	581	978	9.3	17.6	0.59
CG-DP	22.1	9.8	19.4	510	843	9.8	13.5	0.60

stage hardening behavior, as similar to the present CG-DP steel as well as common dual phase steels [8-10]. At the first stage with the low slopes, ferrite matrix deforms plastically but martensite remains elastic. At the second stage with the high slopes, both phases deform plastically. Second, the m values of UFG F/M DP steel was higher than that of CG F/M DP steel at the first stage, but those of both steels at the second stage were comparable. The higher *m* value of UFG F/M DP steel at the first stage would be attributed to the fact that plastic deformation of ferrite in UFG F/M DP steel was more restrained by uniformly distributed surrounding martensite having smaller interspacing compared to CG F/M DP steel [9]. Third, the transition strain (ε_{tr}) between the first and second stages was smaller in UFG F/M DP steel, 2.8%, than that of CG F/M DP steel, 3.7%. That is, plastic deformation of martensite in UFG F/M DP steel started earlier than in CG F/M DP steel, implying that load transfer from ferrite to martensite in the former was more pronounced than that in the latter [10]. The higher m value of UFG F/M DP steel at the first stage lends support to this implication.

4. CONCLUSIONS

1. In order to restore ductility and strain hardenability of UFG steels, UFG V-alloyed steel and UFG F/M DP steel were fabricated by ECAP and various heat treatments.
2. Nano-sized vanadium carbide precipitates in UFG V-alloyed steel with ferrite/pearlite phases was not so effective on improving strain hardenability of that steel.
3. UFG F/M dual phase steel fabricated by a combined process of ECAP and intercritical annealing exhibited an excellent combination of ultrahigh strength, large uniform elongation and extensive strain hardenability.

ACKNOWLEDGEMENT

This work was supported by Ministry of Science and Technology of Korea through 'National Research Laboratory Program'.

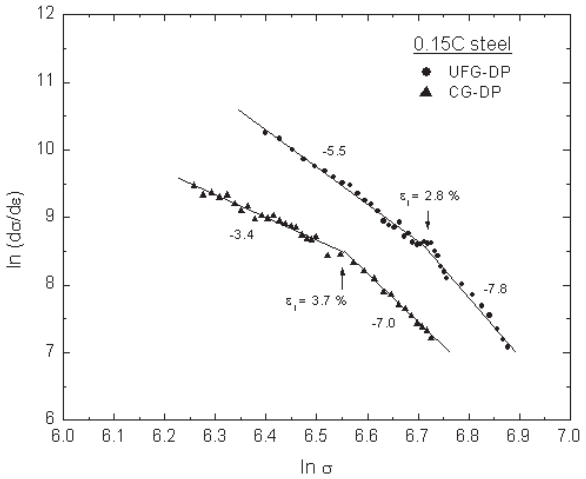

Fig. 5. A plot of the ln($d\sigma/d\varepsilon$) versus lns curve for the modified C-J analysis based on the Swift equation.

REFERENCES

[1] K.-T. Park, Y.S. Kim, J.G. Lee and D.H. Shin // *Mater. Sci. Eng. A* **293** (2000) 165.
[2] Y.M. Wang and E. Ma // *Acta Mater.* **52** (2004) 1699.
[3] C. C. Koch // *Scripta Mater* **49** (2003) 657.
[4] J. Aldazabal and J. Gil Sevillano // *Mater. Sci. Eng. A* **365** (2000) 186.
[5] V.M. Segal // *Mater. Sci. Eng. A* **197** (1995) 157.
[6] R.E. Reed-Hill, W.R. Cribb and S.N. Monteiro // *Metall. Trans. A* **4** (1973) 2665.
[7] H.W. Swift // *J. Mech Phys Solids* **1** (1952) 1.
[8] Y. Tomita and K. Okabayashi // *Metall. Trans. A* **16** (1985) 865.
[9] Z. Jiang , J. Lian and J. Chen // *Mater. Sci. Tech.* **8** (1992) 1075.
[10] Z. Jiang, Z. Guan and Z. Lian // *Mater. Sci. Eng. A* **190** (1995) 55.